Multiobject Tracking with Track Continuity: An Efficient Random Finite Set Based Algorithm

Thomas Kropfreiter and Franz Hlawatsch

***Abstract*—We propose a random finite set (RFS) based algorithm for tracking multiple objects while maintaining track continuity. In our approach, the object states are modeled by a combination of a labeled multi-Bernoulli (LMB) RFS and a Poisson RFS. Low complexity is achieved through several judiciously chosen approximations in the update step. In particular, the computationally less demanding Poisson part of our algorithm is used to track potential objects whose existence is highly uncertain. A new labeled Bernoulli component is generated only if there is sufficient evidence of object existence, and then the corresponding object state is tracked by the more accurate but more complex LMB part of the algorithm. Simulation results for a challenging scenario demonstrate an attractive accuracy-complexity tradeoff and a significant complexity reduction relative to other RFS-based algorithms with comparable performance.**

***Index Terms*—Multiobject tracking, multitarget tracking, labeled multi-Bernoulli process, random finite set, finite point process, track continuity.**

I. Introduction

Multiobject tracking filters recursively estimate the time-dependent number and states of multiple objects from noisy and cluttered sensor measurements. This task is complicated by an unknown association between objects and measurements [1]–[4]. An important class of multiobject tracking filters, which will be considered in this paper, describes both the states and the measurements by random finite sets (RFSs) [4]–[12], also known as finite point processes [13], [14].

In many applications, multiobject tracking filters are required to *maintain track continuity*, i.e., to estimate entire trajectories of consecutive object states. This can be achieved by describing the object states by *labeled* RFSs [4], [7]–[9], [12]. A prominent filter using labeled RFSs is the labeled multi-Bernoulli (LMB) filter [9], in which the multiobject posterior probability density function (pdf) is approximated by an LMB pdf. An alternative filter, which uses RFSs but not labeled RFSs, is the track-oriented marginal multi-Bernoulli/Poisson (TOMB/P) filter [10]. This filter approximates the multiobject posterior pdf by a combination of a multi-Bernoulli pdf and a Poisson pdf. In each time step, a new Bernoulli component is created for each measurement, and Bernoulli components with low existence probabilities are pruned; furthermore, the Poisson RFS supports the creation of new Bernoulli components. A label-augmented version of the TOMB/P filter that maintains track continuity is proposed in [12, Sec. XIII]. A different modification of the TOMB/P filter, presented in [6], transfers Bernoulli components with low existence probability to the Poisson RFS instead of pruning them.

In this paper, we propose a multiobject tracking filter, termed LMB/P filter, that maintains track continuity and is less complex than the LMB filter and the TOMB/P filter and its variants. In the LMB/P filter, the multiobject state is modeled as a tuple of an LMB RFS and a Poisson RFS. The Poisson RFS is used to track potential objects whose existence is highly uncertain. Only if a measure of confidence exceeds a threshold, the LMB/P filter creates a new labeled Bernoulli component—based on the probability hypothesis density (PHD) of the Poisson RFS—and then uses the LMB RFS to track the corresponding potential object. This is different from the TOMB/P filter, which always creates a new labeled Bernoulli component for each measurement. Furthermore, the LMB/P filter transfers certain labeled Bernoulli components back to the Poisson RFS if another measure of confidence falls below a threshold. As a consequence, the LMB/P filter offers a better accuracy-complexity tradeoff than the PHD, LMB, and TOMB/P filters.

The remainder of this paper is organized as follows. In Section II, we review some fundamentals of RFSs. The system model is presented in Section III. Section IV describes the "exact" update step of a hypothetical filter that is based on our system model. The approximate update step performed by the proposed LMB/P filter is presented in Section V. Finally, simulation results are reported in Section VI.

II. Fundamentals of RFSs

An (unlabeled) RFS $\mathsf{X} = \{\mathsf{x}^{(1)}, \dots, \mathsf{x}^{(\mathsf{n})}\}$ is a random variable whose realizations X are—with probability one—finite sets $\{\boldsymbol{x}^{(1)}, \dots, \boldsymbol{x}^{(n)}\}$ of vectors $\boldsymbol{x}^{(i)} \in \mathbb{R}^d$. Both the vectors $\mathsf{x}^{(i)}$ and their number $\mathsf{n} = |\mathsf{X}|$ (the cardinality of X) are random, and the elements $\mathsf{x}^{(i)}$ are unordered. The statistics of an RFS X can be described by the multiobject pdf $f_{\mathsf{X}}(X)$, briefly denoted $f(X)$ [4]. The PHD $D_{\mathsf{X}}(\boldsymbol{x}) : \mathbb{R}^d \to [0, \infty)$ of an RFS X is defined by the fact that for any region $\mathcal{S} \subseteq \mathbb{R}^d$, the integral $\int_{\mathcal{S}} D_{\mathsf{X}}(\boldsymbol{x}) \mathrm{d}\boldsymbol{x}$ yields the expected number of elements $\mathsf{x} \in \mathsf{X}$ that lie in that region. For a *Poisson RFS*, the cardinality $\mathsf{n} = |\mathsf{X}|$ is Poisson distributed with some mean μ. Furthermore, given the cardinality n, the individual elements x are independent and identically distributed (iid) with some vector pdf $f(\boldsymbol{x})$. This yields the multiobject pdf

$$f(X) = e^{-\mu} \prod_{\boldsymbol{x} \in X} \mu f(\boldsymbol{x}) = e^{-\int \lambda(\boldsymbol{x}) \mathrm{d}\boldsymbol{x}} \prod_{\boldsymbol{x} \in X} \lambda(\boldsymbol{x}), \quad (1)$$

T. Kropfreiter and F. Hlawatsch are with the Institute of Telecommunications, TU Wien, Vienna, Austria and with Brno University of Technology, Brno, Czech Republic (e-mail: {thomas.kropfreiter, franz.hlawatsch}@tuwien.ac.at). This work was supported in part by the Austrian Science Fund (FWF) under grant P27370-N30 and by the Czech Science Foundation (GAČR) under grant 17-19638S.

where the product $\lambda(\boldsymbol{x}) \triangleq \mu f(\boldsymbol{x})$ is the PHD of the Poisson RFS. A *Bernoulli RFS* is parametrized by a probability of existence r and a vector pdf $s(\boldsymbol{x})$. It is either empty with probability $1-r$ or contains one element $\mathbf{x} \sim s(\boldsymbol{x})$ with probability r. A *multi-Bernoulli RFS* is the union of a fixed number J of statistically independent Bernoulli RFSs; it is completely specified by the parameter set $\big\{\big(r^{(j)}, s^{(j)}(\boldsymbol{x})\big)\big\}_{j=1}^{J}$.

In a *labeled RFS* $\tilde{\mathsf{X}}$, each element is a tuple of the form $\mathbf{x}^{[\mathrm{l}]} = (\mathbf{x}, \mathrm{l}) \in \mathbb{R}^d \times \mathbb{L}$, where $\mathbb{L}$ is a finite set. The labels of any realization $\tilde{X} = \big\{(\boldsymbol{x}^{(1)}, l^{(1)}), \ldots, (\boldsymbol{x}^{(n)}, l^{(n)})\big\}$ are distinct, i.e., $i \neq j$ implies $l^{(i)} \neq l^{(j)}$. We will denote by $\mathcal{L}(\tilde{X})$ the set of all the labels of $\tilde{X}$. The statistics of a labeled RFS $\tilde{\mathsf{X}}$ can be described by the multiobject pdf $f(\tilde{X})$ [4]. An *LMB RFS* $\tilde{\mathsf{X}}$ is a multi-Bernoulli RFS where the element $\mathbf{x}$ of each Bernoulli component $\mathsf{X}^{(j)}$, $j \in \{1, \ldots, J\}$ is augmented by a distinct label l. Following [4], the same label l is assigned to each state realization $\boldsymbol{x}$ of a given Bernoulli RFS $\mathsf{X}^{(j)}$. To simplify the notation, we index the Bernoulli RFSs directly by their labels l, i.e., we denote them by $\mathsf{X}^{(l)}$, $l \in \mathbb{L}$, with corresponding existence probabilities $r^{(l)}$ and vector pdfs $s^{(l)}(\boldsymbol{x})$ [9]. The multiobject pdf of an LMB RFS $\tilde{\mathsf{X}}$ evaluated for a realization $\tilde{X}$ with cardinality $|\tilde{X}| \leq J$, distinct labels, and label set $\mathcal{L}(\tilde{X}) \subseteq \mathbb{L} = \{l^{(1)}, \ldots, l^{(J)}\}$ (note that $|\mathbb{L}| = J$) is given by [9]

$$f(\tilde{X}) = \prod_{l \in \mathbb{L}} f(\tilde{X}^{(l)}) = \left(\prod_{l' \in \mathbb{L} \setminus \mathcal{L}(\tilde{X})} \big(1 - r^{(l')}\big) \right) \prod_{(\boldsymbol{x}, l) \in \tilde{X}} r^{(l)} s^{(l)}(\boldsymbol{x}). \tag{2}$$

For cardinality $|\tilde{X}| > J$, $f(\tilde{X}) = 0$. The LMB RFS $\tilde{\mathsf{X}}$ is completely specified by the parameter set $\big\{\big(r^{(l)}, s^{(l)}(\boldsymbol{x})\big)\big\}_{l \in \mathbb{L}}$.

III. System Model

We describe the multiobject state at time $k-1$ by the tuple $(\tilde{\mathsf{X}}_{k-1}, \mathsf{X}_{k-1})$, where $\tilde{\mathsf{X}}_{k-1}$ is a labeled RFS with label set $\mathbb{L}_{k-1}$ and X_{k-1} is an unlabeled RFS. We assume that $\tilde{\mathsf{X}}_{k-1}$ and X_{k-1} evolve independently, i.e., $\tilde{\mathsf{X}}_k$ and X_k are conditionally independent given $(\tilde{X}_{k-1}, X_{k-1})$. At time $k-1$, an object with labeled state $\boldsymbol{x}_{k-1}^{[l]} \in \tilde{X}_{k-1}$ (briefly called "labeled object") either survives with probability $p_{\mathrm{S}}\big(\boldsymbol{x}_{k-1}^{[l]}\big)$ or dies with probability $1 - p_{\mathrm{S}}\big(\boldsymbol{x}_{k-1}^{[l]}\big)$. If it survives, its new state $\mathbf{x}_k$ (without the label l) is distributed according to the single-state transition pdf $f\big(\boldsymbol{x}_k \big| \boldsymbol{x}_{k-1}^{[l]}\big)$, and the label is preserved by the state transition. The states of different labeled objects are assumed to evolve independently. Due to these assumptions, the multiobject state of the labeled objects at time k, conditioned on $\tilde{X}_{k-1}$, is described by an LMB RFS $\tilde{\mathsf{X}}_k$ with existence probabilities $p_{\mathrm{S}}\big(\boldsymbol{x}_{k-1}^{[l]}\big)$ and vector pdfs $f\big(\boldsymbol{x}_k \big| \boldsymbol{x}_{k-1}^{[l]}\big)$. Similarly, an object with unlabeled state $\boldsymbol{x}_{k-1} \in X_{k-1}$ (briefly called "unlabeled object") either survives with probability[1] $p_{\mathrm{S}}(\boldsymbol{x}_{k-1})$ or dies with probability $1 - p_{\mathrm{S}}(\boldsymbol{x}_{k-1})$. If it survives, its new state $\mathbf{x}_k$ is distributed according to the single-state transition pdf $f(\boldsymbol{x}_k | \boldsymbol{x}_{k-1})$. The states of different unlabeled objects evolve independently. Thus, the multiobject state of the survived unlabeled objects at time k, conditioned on X_{k-1}, is described by a multi-Bernoulli RFS $\mathsf{X}_k^{\mathrm{S}}$ with existence probabilities $p_{\mathrm{S}}(\boldsymbol{x}_{k-1})$ and vector pdfs $f(\boldsymbol{x}_k | \boldsymbol{x}_{k-1})$. Finally, the multiobject state of newborn (unlabeled) objects is modeled as a Poisson RFS $\mathsf{X}_k^{\mathrm{B}}$ with mean parameter μ_{B} and vector pdf $f_{\mathrm{B}}(\boldsymbol{x}_k)$ and, hence, PHD $\lambda_{\mathrm{B}}(\boldsymbol{x}_k) = \mu_{\mathrm{B}} f_{\mathrm{B}}(\boldsymbol{x}_k)$. Thus, the entirety of unlabeled objects at time k, given X_{k-1}, is described by the RFS $\mathsf{X}_k = \mathsf{X}_k^{\mathrm{S}} \cup \mathsf{X}_k^{\mathrm{B}}$.

At time k, a sensor produces M_k measurements $\mathbf{z}_k^{(1)}, \ldots, \mathbf{z}_k^{(\mathsf{M}_k)}$, which are described by an (unlabeled) RFS $\mathsf{Z}_k \triangleq \big\{\mathbf{z}_k^{(1)}, \ldots, \mathbf{z}_k^{(\mathsf{M}_k)}\big\}$. The measurements may originate from a labeled object, an unlabeled object, or clutter. A labeled object with state $\boldsymbol{x}_k^{[l]} \in \tilde{X}_k$ is detected—i.e., it generates a measurement—with probability $p_{\mathrm{D}}\big(\boldsymbol{x}_k^{[l]}\big)$, or is missed—i.e., it does not generate a measurement—with probability $1 - p_{\mathrm{D}}\big(\boldsymbol{x}_k^{[l]}\big)$. If it is detected, it generates one measurement $\mathbf{z}_k$, which is distributed according to the single-object likelihood function $f\big(\boldsymbol{z}_k \big| \boldsymbol{x}_k^{[l]}\big)$. We assume that $\mathbf{z}_k$ is conditionally independent, given $\boldsymbol{x}_k^{[l]}$, of all the other measurements and object states. Accordingly, the measurements originating from labeled objects are described by a multi-Bernoulli RFS $\mathsf{Z}_k^{\mathrm{L}}$ with parameter set $\big\{\big(p_{\mathrm{D}}\big(\boldsymbol{x}_k^{[l]}\big), f\big(\boldsymbol{z}_k \big| \boldsymbol{x}_k^{[l]}\big)\big)\big\}_{l \in \mathbb{L}_{k-1}}$. Similarly, an unlabeled object with state $\boldsymbol{x}_k \in X_k$ is detected with probability[2] $p_{\mathrm{D}}(\boldsymbol{x}_k)$ or missed with probability $1 - p_{\mathrm{D}}(\boldsymbol{x}_k)$. If it is detected, it generates one measurement $\mathbf{z}_k$ that is distributed according to the single-object likelihood function $f(\boldsymbol{z}_k | \boldsymbol{x}_k)$. We assume that $\mathbf{z}_k$ is conditionally independent, given $\boldsymbol{x}_k$, of all the other measurements and object states. Thus, the measurements originating from unlabeled objects are described by a multi-Bernoulli RFS $\mathsf{Z}_k^{\mathrm{U}}$ with parameter set $\big\{\big(p_{\mathrm{D}}(\boldsymbol{x}_k), f(\boldsymbol{z}_k | \boldsymbol{x}_k)\big)\big\}_{\boldsymbol{x}_k \in X_k}$. Finally, the clutter-originated measurements are described by a Poisson RFS $\mathsf{Z}_k^{\mathrm{C}}$ with mean parameter μ_{C} and vector pdf $f_{\mathrm{C}}(\boldsymbol{z}_k)$ and, hence, PHD $\lambda_{\mathrm{C}}(\boldsymbol{z}_k) = \mu_{\mathrm{C}} f_{\mathrm{C}}(\boldsymbol{z}_k)$. It thus follows that the overall measurement RFS at time k is $\mathsf{Z}_k = \mathsf{Z}_k^{\mathrm{L}} \cup \mathsf{Z}_k^{\mathrm{U}} \cup \mathsf{Z}_k^{\mathrm{C}}$. Here, $\mathsf{Z}_k^{\mathrm{L}}$, $\mathsf{Z}_k^{\mathrm{U}}$, and $\mathsf{Z}_k^{\mathrm{C}}$ are assumed to be conditionally independent given $(\tilde{X}_k, X_k)$.

IV. Exact Update Step

Let $Z_{1:k} \triangleq (Z_1, \ldots, Z_k)$ denote the ordered list of all the measurements up to time k. Our goal is to estimate the multiobject state $(\tilde{\mathsf{X}}_k, \mathsf{X}_k)$ from $Z_{1:k}$ in a time-sequential (recursive) manner. To this end, the proposed LMB/P filter propagates an approximation of the posterior multiobject pdf $f(\tilde{X}_k, X_k | Z_{1:k})$ from one time step to the next. First, in a prediction step, an approximation of the preceding posterior pdf $f(\tilde{X}_{k-1}, X_{k-1} | Z_{1:k-1})$ is converted into an approximation of the "predicted" posterior pdf $f(\tilde{X}_k, X_k | Z_{1:k-1})$. Next, in an update step, this latter approximation is converted into an approximation of the new posterior pdf $f(\tilde{X}_k, X_k | Z_{1:k})$.

To derive the LMB/P filter, we model $\tilde{\mathsf{X}}_{k-1}$ by an LMB RFS and X_{k-1} by a Poisson RFS. The LMB RFS consists of $|\mathbb{L}_{k-1}|$ labeled Bernoulli components with existence probabilities $r_{k-1}^{(l)}$ and vector pdfs $s^{(l)}(\boldsymbol{x}_{k-1})$, with $l \in \mathbb{L}_{k-1}$. The Poisson RFS is parametrized by the posterior PHD

[1] With an abuse of notation, $p_{\mathrm{S}}(\cdot)$ is used to denote both the survival probability of labeled objects (with argument $\boldsymbol{x}_{k-1}^{[l]}$) and of unlabeled objects (with argument $\boldsymbol{x}_{k-1}$).

[2] Similarly to $p_{\mathrm{S}}(\cdot)$, we denote by $p_{\mathrm{D}}(\cdot)$ both the detection probability of labeled objects (with argument $\boldsymbol{x}_k^{[l]}$) and of unlabeled objects (with argument $\boldsymbol{x}_k$).

$\lambda(\boldsymbol{x}_{k-1})$. We assume that $\tilde{\mathsf{X}}_{k-1}$ and X_{k-1} are conditionally independent given all the measurements up to time $k-1$, i.e., $f(\tilde{X}_{k-1}, X_{k-1}|Z_{1:k-1}) = f(\tilde{X}_{k-1}|Z_{1:k-1})\, f(X_{k-1}|Z_{1:k-1})$.

The prediction step is a straightforward extension (incorporating labels) of the prediction step of the TOMB/P filter [10] and will not be presented here because of space limitations. The predicted posterior pdf is obtained as $f(\tilde{X}_k, X_k|Z_{1:k-1}) = f(\tilde{X}_k|Z_{1:k-1})\, f(X_k|Z_{1:k-1})$, where $f(\tilde{X}_k|Z_{1:k-1})$ is an LMB pdf parametrized by existence probabilities $r^{(l)}_{k|k-1}$ and vector pdfs $s^{(l)}_{k|k-1}(\boldsymbol{x}_k)$, with $l \in \mathbb{L}_{k-1}$, and $f(X_k|Z_{1:k-1})$ is (by virtue of an approximation) a Poisson pdf parametrized by the PHD $\lambda_{k|k-1}(\boldsymbol{x}_k)$. Expressions of these parameters can be found in [10].

The "exact" update step for our system model is again a straightforward extension (incorporating labels) of the update step in [10]. The posterior pdf is obtained as $f(\tilde{X}_k, X_k|Z_{1:k}) = f(\tilde{X}_k|Z_{1:k})\, f(X_k|Z_{1:k})$, where $f(\tilde{X}_k|Z_{1:k})$ is the pdf of an *LMB mixture* (LMBM) and $f(X_k|Z_{1:k})$ is a Poisson pdf. Expressions of these pdfs or their parameters will be presented in the following; they will provide a basis for developing the "approximate" update step of the LMB/P filter in Section V.

A. Exact Update Step for the Labeled Objects

We first discuss the posterior pdf of the labeled objects, $f(\tilde{X}_k|Z_{1:k})$. The label set $\mathbb{L}_k$ of $\tilde{\mathsf{X}}_k$ evolves as $\mathbb{L}_k = \mathbb{L}_{k-1} \cup \mathbb{L}^{\text{new}}_k$, where $\mathbb{L}_{k-1} \cap \mathbb{L}^{\text{new}}_k = \emptyset$. Here, the labels $l \in \mathbb{L}_{k-1}$ represent "legacy" Bernoulli components, which already existed at time $k-1$, and the labels $l \equiv (k,m) \in \mathbb{L}^{\text{new}}_k$ represent new Bernoulli components, of which one is created for each measurement $\boldsymbol{z}^{(m)}_k$, $m \in \{1,\dots,M_k\}$. Note that, as a consequence, $|\mathbb{L}^{\text{new}}_k| = |Z_k| = M_k$.

Consider the *association vector* $\mathbf{a}_k = \big[\mathsf{a}^{(1)}_k \cdots \mathsf{a}^{(|\mathbb{L}_k|)}_k\big]^{\mathrm{T}}$ with entries $\mathsf{a}^{(l)}_k$ defined as follows. For $l \in \mathbb{L}_{k-1}$, $\mathsf{a}^{(l)}_k = m \in \{1,\dots,M_k\}$ indicates that the labeled object with state $\boldsymbol{x}^{[l]}_k$ generates measurement $\boldsymbol{z}^{(m)}_k$, whereas $\mathsf{a}^{(l)}_k = 0$ indicates that it does not generate a measurement. For $l \equiv (k,m) \in \mathbb{L}^{\text{new}}_k$, $\mathsf{a}^{(l)}_k = \mathsf{a}^{(k,m)}_k = 1$ indicates that the labeled object with state $\boldsymbol{x}^{[l=(k,m)]}_k$ generates $\boldsymbol{z}^{(m)}_k$, whereas $\mathsf{a}^{(k,m)}_k = 0$ indicates that it does not generate a measurement. Note that $\mathbf{a}_k \in \{0,\dots,M_k\}^{|\mathbb{L}_{k-1}|} \times \{0,1\}^{|\mathbb{L}^{\text{new}}_k|}$ with $|\mathbb{L}^{\text{new}}_k| = M_k$. We call each possible value $\boldsymbol{a}_k$ of $\mathbf{a}_k$ a *global association hypothesis*. Furthermore, we call $\boldsymbol{a}_k$ *admissible* if at most one measurement is assigned to the same labeled object and no measurement is assigned to more than one labeled object, i.e., if the nonzero entries $a^{(l)}_k$ are all different. We denote by $\mathcal{A}_k$ the set of all admissible $\boldsymbol{a}_k$. A derivation analogous to [10] now shows that $f(\tilde{X}_k|Z_{1:k})$ is an LMBM pdf, i.e.,

$$f(\tilde{X}_k|Z_{1:k}) = \sum_{\boldsymbol{a}_k \in \mathcal{A}_k} w_{\boldsymbol{a}_k} f^{(\boldsymbol{a}_k)}(\tilde{X}_k). \tag{3}$$

Here, $f^{(\boldsymbol{a}_k)}(\tilde{X}_k) = \prod_{l\in\mathbb{L}_k} f^{(l,a^{(l)}_k)}(\tilde{X}^{(l)}_k)$ is an LMB pdf (cf. (2)) parametrized by $\big\{\big(r^{(l,a^{(l)}_k)}_k, s^{(l,a^{(l)}_k)}(\boldsymbol{x}_k)\big)\big\}_{l\in\mathbb{L}_k}$, and the weights $w_{\boldsymbol{a}_k}$ are given by

$$w_{\boldsymbol{a}_k} = \frac{1}{B_k} \prod_{l\in\mathbb{L}_k} \beta^{(l,a^{(l)}_k)}_k, \tag{4}$$

where $B_k = \sum_{\boldsymbol{a}_k\in\mathcal{A}_k} \prod_{l\in\mathbb{L}_k} \beta^{(l,a^{(l)}_k)}_k$ is a normalization factor. The factors $\beta^{(l,a^{(l)}_k)}_k$ are known as *association weights* [10].

The parameters $\beta^{(l,a^{(l)}_k)}_k$, $r^{(l,a^{(l)}_k)}_k$, and $s^{(l,a^{(l)}_k)}(\boldsymbol{x}_k)$ are given as follows [10]. We first consider $l \in \mathbb{L}_{k-1}$. For $a^{(l)}_k = m \in \{1,\dots,M_k\}$, we have

$$\beta^{(l,m)}_k = r^{(l)}_{k|k-1}\, c^{(l,m)}_k, \tag{5}$$

$$r^{(l,m)}_k = 1, \tag{6}$$

$$s^{(l,m)}(\boldsymbol{x}_k) = \frac{p_{\mathrm{D}}\big(\boldsymbol{x}^{[l]}_k\big)\, f\big(\boldsymbol{z}^{(m)}_k\big|\boldsymbol{x}^{[l]}_k\big)\, s^{(l)}_{k|k-1}(\boldsymbol{x}_k)}{c^{(l,m)}_k}, \tag{7}$$

with $c^{(l,m)}_k = \int p_{\mathrm{D}}\big(\boldsymbol{x}^{[l]}_k\big)\, f\big(\boldsymbol{z}^{(m)}_k\big|\boldsymbol{x}^{[l]}_k\big)\, s^{(l)}_{k|k-1}(\boldsymbol{x}_k)\,\mathrm{d}\boldsymbol{x}_k$, and for $a^{(l)}_k = 0$, we have

$$\beta^{(l,0)}_k = 1 - r^{(l)}_{k|k-1} + r^{(l)}_{k|k-1} d^{(l)}_k, \tag{8}$$

$$r^{(l,0)}_k = \frac{r^{(l)}_{k|k-1} d^{(l)}_k}{\beta^{(l,0)}_k}, \tag{9}$$

$$s^{(l,0)}(\boldsymbol{x}_k) = \frac{\big(1 - p_{\mathrm{D}}\big(\boldsymbol{x}^{[l]}_k\big)\big)\, s^{(l)}_{k|k-1}(\boldsymbol{x}_k)}{d^{(l)}_k}, \tag{10}$$

with $d^{(l)}_k = \int \big(1 - p_{\mathrm{D}}\big(\boldsymbol{x}^{[l]}_k\big)\big)\, s^{(l)}_{k|k-1}(\boldsymbol{x}_k)\,\mathrm{d}\boldsymbol{x}_k$. Next, we consider $l \equiv (k,m) \in \mathbb{L}^{\text{new}}_k$. For $a^{(l)}_k = 1$, we have

$$\beta^{(l=(k,m),1)}_k = \lambda_{\mathrm{C}}\big(\boldsymbol{z}^{(m)}_k\big) + \omega^{(m)}_k, \tag{11}$$

$$r^{(l=(k,m),1)}_k = \frac{\omega^{(m)}_k}{\beta^{(l=(k,m),1)}_k}, \tag{12}$$

$$s^{(l=(k,m),1)}(\boldsymbol{x}_k) = \frac{p_{\mathrm{D}}(\boldsymbol{x}_k)\, f\big(\boldsymbol{z}^{(m)}_k\big|\boldsymbol{x}_k\big)\, \lambda_{k|k-1}(\boldsymbol{x}_k)}{\omega^{(m)}_k}, \tag{13}$$

with $\omega^{(m)}_k = \int p_{\mathrm{D}}(\boldsymbol{x}_k)\, f\big(\boldsymbol{z}^{(m)}_k\big|\boldsymbol{x}_k\big)\, \lambda_{k|k-1}(\boldsymbol{x}_k)\,\mathrm{d}\boldsymbol{x}_k$, and for $a^{(l)}_k = 0$, we have $\beta^{(l=(k,m),0)}_k = 1$ and $r^{(l=(k,m),0)}_k = 0$. (Note that $s^{(l=(k,m),0)}(\boldsymbol{x}_k)$ is not defined since $r^{(l=(k,m),0)}_k = 0$ implies that the object with label l does not exist.)

B. Exact Update Step for the Unlabeled Objects

For the posterior pdf of the unlabeled objects, $f(X_k|Z_{1:k})$, a derivation analogous to [10] yields the Poisson pdf (cf. (1))

$$f(X_k|Z_{1:k}) = e^{-\int \lambda(\boldsymbol{x}_k)\,\mathrm{d}\boldsymbol{x}_k} \prod_{\boldsymbol{x}_k \in X_k} \lambda(\boldsymbol{x}_k), \tag{14}$$

where $\lambda(\boldsymbol{x}_k)$, the updated posterior PHD, is given by

$$\lambda(\boldsymbol{x}_k) = (1 - p_{\mathrm{D}}(\boldsymbol{x}_k))\, \lambda_{k|k-1}(\boldsymbol{x}_k). \tag{15}$$

V. Approximate Update Step

The proposed LMB/P filter is derived by a two-stage approximation of the exact update step discussed above. In the first stage, $f(\tilde{X}_k, X_k|Z_{1:k})$ is approximated by the product of an LMBM pdf of smaller complexity than $f(\tilde{X}_k|Z_{1:k})$ in (3) and a pdf that is the set convolution [4] of a multi-Bernoulli pdf and a Poisson pdf. In the second stage, the LMBM pdf is approximated by an LMB pdf and the multi-Bernoulli/Poisson convolution pdf is approximated by a Poisson pdf.

A. First Approximation Stage

The first approximation is based on the following partitionings of the label set $\mathbb{L}_k$ and of the measurement set Z_k. We first partition the label set of the legacy Bernoulli components as $\mathbb{L}_{k-1} = \mathbb{L}^*_{k-1} \cup \bar{\mathbb{L}}^*_{k-1}$, with $\mathbb{L}^*_{k-1} \cap \bar{\mathbb{L}}^*_{k-1} = \emptyset$. Here, $\mathbb{L}^*_{k-1}$ consists of all $l \in \mathbb{L}_{k-1}$ for which $\beta_k^{(l,m)} r_k^{(l,m)} \geq \gamma$ for some $m \in \{0, \ldots, M_k\}$, with a positive threshold γ, and $\bar{\mathbb{L}}^*_{k-1} = \mathbb{L}_{k-1} \setminus \mathbb{L}^*_{k-1}$. The product $\beta_k^{(l,m)} r_k^{(l,m)}$ is a "measure of confidence" that the labeled object with state $\boldsymbol{x}_k^{[l]}$, $l \in \mathbb{L}_{k-1}$ exists and is associated with measurement $\boldsymbol{z}_k^{(m)}$ (if $m \in \{1, \ldots, M_k\}$) or is missed (if $m = 0$).

We also partition the set of measurements as $Z_k = Z_k^* \cup \bar{Z}_k^*$, with $Z_k^* \cap \bar{Z}_k^* = \emptyset$. Here, Z_k^* consists of all measurements $\boldsymbol{z}_k^{(m)}$, $m \in \{1, \ldots, M_k\}$ for which $\beta_k^{(l,m)} r_k^{(l,m)} \geq \gamma_{\text{leg}}$ for some $l \in \mathbb{L}^*_{k-1}$ and of all measurements $\boldsymbol{z}_k^{(m)}$, $m \in \{1, \ldots, M_k\}$ corresponding to $l \equiv (k,m) \in \mathbb{L}_k^{\text{new}}$ for which $\beta_k^{(l=(k,m),1)} r_k^{(l=(k,m),1)} \geq \gamma_{\text{new}}$, with two further positive thresholds γ_{leg} and γ_{new}. The partitioning $Z_k = Z_k^* \cup \bar{Z}_k^*$ corresponds to a partitioning of the set of measurement indices m as $\{1, \ldots, M_k\} = \mathcal{M}_k^* \cup \bar{\mathcal{M}}_k^*$, with $\mathcal{M}_k^* \cap \bar{\mathcal{M}}_k^* = \emptyset$. According to the above definition of Z_k^*, the measurements in Z_k^* (with indices $m \in \mathcal{M}_k^*$) are likely to originate from some objects with labels $l \in \mathbb{L}^*_{k-1} \cup \mathbb{L}_k^{\text{new}}$.

Since each measurement $\boldsymbol{z}_k \in Z_k$ corresponds to a new Bernoulli component $l \in \mathbb{L}_k^{\text{new}}$, the partitioning $Z_k = Z_k^* \cup \bar{Z}_k^*$ also corresponds to a partitioning of the label set $\mathbb{L}_k^{\text{new}}$ as $\mathbb{L}_k^{\text{new}} = \mathbb{L}_k^{\text{new}*} \cup \bar{\mathbb{L}}_k^{\text{new}*}$, with $\mathbb{L}_k^{\text{new}*} \cap \bar{\mathbb{L}}_k^{\text{new}*} = \emptyset$. Here, $\mathbb{L}_k^{\text{new}*}$ and $\bar{\mathbb{L}}_k^{\text{new}*}$ correspond to Z_k^* and $\bar{Z}_k^*$, respectively. Finally, combining the above partitionings of $\mathbb{L}_{k-1}$ and $\mathbb{L}_k^{\text{new}}$ with our earlier partitioning $\mathbb{L}_k = \mathbb{L}_{k-1} \cup \mathbb{L}_k^{\text{new}}$ yields $\mathbb{L}_k = \mathbb{L}^*_{k-1} \cup \bar{\mathbb{L}}^*_{k-1} \cup \mathbb{L}_k^{\text{new}*} \cup \bar{\mathbb{L}}_k^{\text{new}*}$. We note that our partitioning scheme is different from the grouping procedure used in the LMB filter [9]; in particular, the LMB filter partitions labeled objects and measurements that are likely to originate from them based on the Mahalanobis distance.

The first approximation is now obtained by pruning in (3) unlikely associations $\boldsymbol{a}_k$. More specifically, these associations are chosen as those $\boldsymbol{a}_k \in \mathcal{A}_k$ that contain one or several associations of labeled states $\boldsymbol{x}_k^{[l]}$, $l \in \bar{\mathbb{L}}^*_{k-1}$ with measurements $\boldsymbol{z}_k^{(m)}$, $m \in \{1, \ldots, M_k\}$ and those $\boldsymbol{a}_k \in \mathcal{A}_k$ that do not associate each $\boldsymbol{x}_k^{[l]}$, $l \equiv (k,m) \in \bar{\mathbb{L}}_k^{\text{new}*}$ with some $\boldsymbol{z}_k^{(m)}$, $m \in \bar{\mathcal{M}}_k^*$. It can be shown that this pruning results in an approximation of the exact posterior pdf $f(\tilde{X}_k, X_k|Z_{1:k})$ by

$$f'(\tilde{X}_k, X_k|Z_{1:k}) = f'(\tilde{X}_k|Z_{1:k})\, f'(X_k|Z_{1:k}) . \tag{16}$$

The first factor, $f'(\tilde{X}_k|Z_{1:k})$, is an LMBM pdf of lower complexity than (3), given by

$$f'(\tilde{X}_k|Z_{1:k}) = \sum_{\boldsymbol{a}'_k \in \mathcal{A}'_k} w_{\boldsymbol{a}'_k} f^{(\boldsymbol{a}'_k)}(\tilde{X}_k) . \tag{17}$$

Here, $\mathsf{a}'_k = \big[\mathsf{a}_k^{(1)\prime} \cdots \mathsf{a}_k^{(|\mathbb{L}'_k|)\prime}\big]^{\mathrm{T}}$, where $\mathbb{L}'_k \triangleq \mathbb{L}^*_{k-1} \cup \mathbb{L}_k^{\text{new}*}$ and the entries $\mathsf{a}_k^{(l)\prime}$ are as follows (cf. Section IV-A). For $l \in \mathbb{L}^*_{k-1}$, $\mathsf{a}_k^{(l)\prime} = m \in \mathcal{M}_k^*$ indicates that the labeled object with state $\boldsymbol{x}_k^{[l]}$ generates $\boldsymbol{z}_k^{(m)}$, whereas $\mathsf{a}_k^{(l)\prime} = 0$ indicates that it does not generate a measurement. For $l \equiv (k,m) \in \mathbb{L}_k^{\text{new}*}$, $\mathsf{a}_k^{(l)\prime} = \mathsf{a}_k^{(k,m)\prime} = 1$ indicates that the labeled object with state $\boldsymbol{x}_k^{[l=(k,m)]}$ generates $\boldsymbol{z}_k^{(m)}$, whereas $\mathsf{a}_k^{(k,m)\prime} = 0$ indicates that it does not generate a measurement. Thus, $\mathsf{a}'_k \in (\{0\} \cup \mathcal{M}_k^*)^{|\mathbb{L}^*_{k-1}|} \times \{0,1\}^{|\mathbb{L}_k^{\text{new}*}|}$. Furthermore, $\mathcal{A}'_k$ in (17) is a reduced association alphabet that comprises all the admissible $\boldsymbol{a}'_k$, i.e., those whose nonzero entries $a_k^{(l)\prime}$ are all different. Finally, the $f^{(\boldsymbol{a}'_k)}(\tilde{X}_k)$ are LMB pdfs parametrized by $\big\{\big(r_k^{(l,a_k^{(l)\prime})}, s^{(l,a_k^{(l)\prime})}(\boldsymbol{x}_k)\big)\big\}_{l \in \mathbb{L}'_k}$, and (cf. (4))

$$w_{\boldsymbol{a}'_k} = \frac{1}{B'_k} \prod_{l \in \mathbb{L}'_k} \beta_k^{(l,a_k^{(l)\prime})}, \tag{18}$$

with $B'_k = \sum_{\boldsymbol{a}'_k \in \mathcal{A}'_k} \prod_{l \in \mathbb{L}'_k} \beta_k^{(l,a_k^{(l)\prime})}$. Here, $\beta_k^{(l,a_k^{(l)\prime})}$, $r_k^{(l,a_k^{(l)\prime})}$, and $s^{(l,a_k^{(l)\prime})}(\boldsymbol{x}_k)$ are given for $l \in \mathbb{L}^*_{k-1}$ by (5)–(7) if $a_k^{(l)\prime} = m \in \mathcal{M}_k^*$ and by (8)–(10) if $a_k^{(l)\prime} = 0$, and for $l \equiv (k,m) \in \mathbb{L}_k^{\text{new}*}$ by (11)–(13) if $a_k^{(l)\prime} = 1$ and by $\beta_k^{(l=(k,m),0)} = 1$ and $r_k^{(l=(k,m),0)} = 0$ (and $s^{(l=(k,m),0)}(\boldsymbol{x}_k)$ undefined) if $a_k^{(l)\prime} = 0$.

The second factor in (16), $f'(X_k|Z_{1:k})$, is the set convolution [4] of a multi-Bernoulli pdf and a Poisson pdf. The multi-Bernoulli pdf is parametrized by $\big\{\big(r_k^{(l,0)}, s^{(l,0)}(\boldsymbol{x}_k)\big)\big\}_{l \in \bar{\mathbb{L}}^*_{k-1}}$ and $\big\{\big(r_k^{(l=(k,m),1)}, s^{(l=(k,m),1)}(\boldsymbol{x}_k)\big)\big\}_{m \in \bar{\mathcal{M}}_k^*}$, where $m \in \bar{\mathcal{M}}_k^*$ corresponds to $l \equiv (k,m) \in \bar{\mathbb{L}}_k^{\text{new}*}$. Here, $r_k^{(l,0)}$ and $s^{(l,0)}(\boldsymbol{x}_k)$ are given by (9) and (10), respectively, and $r_k^{(l=(k,m),1)}$ and $s^{(l=(k,m),1)}(\boldsymbol{x}_k)$ by (12) and (13), respectively. The Poisson pdf is as in the exact update step, and thus given by (14), (15).

B. Second Approximation Stage

In the second approximation stage, the LMBM pdf $f'(\tilde{X}_k|Z_{1:k})$ is approximated by an LMB pdf $\tilde{f}(\tilde{X}_k|Z_{1:k})$ and the multi-Bernoulli/Poisson convolution pdf $f'(X_k|Z_{1:k})$ is approximated by a Poisson pdf $\tilde{f}(X_k|Z_{1:k})$. The LMB approximation of $f'(\tilde{X}_k|Z_{1:k})$ is based on formally interpreting the weights $w_{\boldsymbol{a}'_k}$ in (17), (18) as the probability mass function (pmf) of a'_k, i.e., setting $p(\boldsymbol{a}'_k) \triangleq w_{\boldsymbol{a}'_k}$ for $\boldsymbol{a}'_k \in \mathcal{A}'_k$ and $p(\boldsymbol{a}'_k) \triangleq 0$ otherwise. Expression (17) can then be rewritten as

$$f'(\tilde{X}_k|Z_{1:k}) = \sum_{\boldsymbol{a}'_k \in \tilde{\mathcal{A}}_k} p(\boldsymbol{a}'_k) f^{(\boldsymbol{a}'_k)}(\tilde{X}_k) , \tag{19}$$

where $\tilde{\mathcal{A}}_k \triangleq (\{0\} \cup \mathcal{M}_k^*)^{|\mathbb{L}^*_{k-1}|} \times \{0,1\}^{|\mathbb{L}_k^{\text{new}*}|}$. Note that although the summation set $\tilde{\mathcal{A}}_k$ is larger than $\mathcal{A}'_k$ in (17), Eq. (19) is equivalent to (17) because $p(\boldsymbol{a}'_k) = 0$ for $\boldsymbol{a}'_k \in \tilde{\mathcal{A}}_k \setminus \mathcal{A}'_k$.

Following [10], we now "approximate" $p(\boldsymbol{a}'_k)$ by the product of the marginal pmfs $p\big(a_k^{(l)\prime}\big)$, i.e.,

$$p(\boldsymbol{a}'_k) \approx p'(\boldsymbol{a}'_k) \triangleq \prod_{l \in \mathbb{L}'_k} p\big(a_k^{(l)\prime}\big) , \quad \boldsymbol{a}'_k \in \tilde{\mathcal{A}}_k ,$$

where

$$p\big(a_k^{(l)\prime}\big) \triangleq \begin{cases} \sum_{\boldsymbol{a}'^{\sim l}_k \in \tilde{\mathcal{A}}_k^{\text{leg}}} p(\boldsymbol{a}'_k) , & l \in \mathbb{L}^*_{k-1} \\ \sum_{\boldsymbol{a}'^{\sim l}_k \in \tilde{\mathcal{A}}_k^{\text{new}}} p(\boldsymbol{a}'_k) , & l \in \mathbb{L}_k^{\text{new}*} \end{cases} \tag{20}$$

(recall that $\mathbb{L}'_k = \mathbb{L}^*_{k-1} \cup \mathbb{L}_k^{\text{new}*}$). In (20), $\boldsymbol{a}'^{\sim l}_k$ denotes the vector $\boldsymbol{a}'_k$ with the lth component, $a_k^{(l)\prime}$, removed, and the summation sets are $\tilde{\mathcal{A}}_k^{\text{leg}} \triangleq (\{0\} \cup \mathcal{M}_k^*)^{|\mathbb{L}_{k-1}^*|-1} \times \{0,1\}^{|\mathbb{L}_k^{\text{new}*}|}$ and $\tilde{\mathcal{A}}_k^{\text{new}} \triangleq (\{0\} \cup \mathcal{M}_k^*)^{|\mathbb{L}_{k-1}^*|} \times \{0,1\}^{|\mathbb{L}_k^{\text{new}*}|-1}$. Substituting $p'(\boldsymbol{a}_k')$ for $p(\boldsymbol{a}_k')$ in (19) and using $f^{(\boldsymbol{a}_k')}(\tilde{X}_k) = \prod_{l\in\mathbb{L}_k'} f^{(l,a_k^{(l)\prime})}(\tilde{X}_k^{(l)})$ (cf. (2)) yields

$$\begin{aligned}\tilde{f}(\tilde{X}_k|Z_{1:k}) &\triangleq \sum_{\boldsymbol{a}_k'\in\tilde{\mathcal{A}}_k} \prod_{l\in\mathbb{L}_k'} p\big(a_k^{(l)\prime}\big) f^{(l,a_k^{(l)\prime})}(\tilde{X}_k^{(l)}) \\ &= \Bigg(\prod_{l\in\mathbb{L}_{k-1}} \sum_{a_k^{(l)\prime}\in\{0\}\cup\mathcal{M}_k^*} p\big(a_k^{(l)\prime}\big) f^{(l,a_k^{(l)\prime})}(\tilde{X}_k^{(l)})\Bigg) \\ &\quad\times \prod_{l\in\mathbb{L}_k^{\text{new}*}} \sum_{a_k^{(l)\prime}\in\{0,1\}} p\big(a_k^{(l)\prime}\big) f^{(l,a_k^{(l)\prime})}(\tilde{X}_k^{(l)}) . \end{aligned} \tag{21}$$

This can be shown to be an LMB pdf $\tilde{f}(\tilde{X}_k|Z_{1:k}) = \prod_{l\in\mathbb{L}_k'} f(\tilde{X}_k^{(l)})$, where $f(\tilde{X}_k^{(l)})$ is a labeled Bernoulli pdf with parameters

$$r_k^{(l)} = \begin{cases} \sum_{a_k^{(l)\prime}\in\{0\}\cup\mathcal{M}_k^*} p\big(a_k^{(l)\prime}\big) r_k^{(l,a_k^{(l)\prime})}, & l\in\mathbb{L}_{k-1}^* , \\ p\big(a_k^{(l)\prime}\!=\!1\big) r_k^{(l,a_k^{(l)\prime}=1)}, & l\in\mathbb{L}_k^{\text{new}*}, \end{cases} \tag{22}$$

$$s^{(l)}(\boldsymbol{x}_k) = \begin{cases} \frac{1}{r_k^{(l)}} \sum_{a_k^{(l)\prime}\in\{0\}\cup\mathcal{M}_k^*} p\big(a_k^{(l)\prime}\big) r_k^{(l,a_k^{(l)\prime})} s^{(l,a_k^{(l)\prime})}(\boldsymbol{x}_k), \\ \qquad\qquad l\in\mathbb{L}_{k-1}^* , \\ s^{(l,a_k^{(l)\prime}=1)}(\boldsymbol{x}_k), \qquad l\in\mathbb{L}_k^{\text{new}*}. \end{cases} \tag{23}$$

Note that $\mathbb{L}_{k-1}^*$ depends on γ and $\mathbb{L}_k^{\text{new}*}$ depends on γ_{leg} and γ_{new}.

Next, we approximate $f'(X_k|Z_{1:k})$ in (16) by a Poisson pdf

$$\tilde{f}(X_k|Z_{1:k}) \triangleq e^{-\int\tilde{\lambda}(\boldsymbol{x}_k)\mathrm{d}\boldsymbol{x}_k} \prod_{\boldsymbol{x}_k\in X_k} \tilde{\lambda}(\boldsymbol{x}_k), \tag{24}$$

where the PHD $\tilde{\lambda}(\boldsymbol{x}_k)$ is chosen equal to the PHD corresponding to $f'(X_k|Z_{1:k})$. One can show that

$$\begin{aligned}&\tilde{\lambda}(\boldsymbol{x}_k) \\ &= \sum_{l\in\bar{\mathbb{L}}_{k-1}^*} r_k^{(l,0)} s^{(l,0)}(\boldsymbol{x}_k) + \sum_{m\in\bar{\mathcal{M}}_k^*} r_k^{(l=(k,m),1)} s^{(l=(k,m),1)}(\boldsymbol{x}_k) \\ &\quad + \big(1-p_{\text{D}}(\boldsymbol{x}_k)\big)\lambda_{k|k-1}(\boldsymbol{x}_k). \end{aligned} \tag{25}$$

Here, $\sum_{l\in\bar{\mathbb{L}}_{k-1}^*} r_k^{(l,0)} s^{(l,0)}(\boldsymbol{x}_k)$ corresponds to labeled objects that are unlikely to exist; the corresponding labeled Bernoulli components are thereby transferred back to the Poisson RFS. Furthermore, $\sum_{m\in\bar{\mathcal{M}}_k^*} r_k^{(l=(k,m),1)} s^{(l=(k,m),1)}(\boldsymbol{x}_k)$ corresponds to measurements that are not likely to originate from any labeled object. Finally, $\big(1-p_{\text{D}}(\boldsymbol{x}_k)\big)\lambda_{k|k-1}(\boldsymbol{x}_k)$ corresponds to unlabeled objects that are undetected. Note that $\bar{\mathbb{L}}_{k-1}^*$ depends on γ and $\bar{\mathcal{M}}_k^*$ depends on γ_{leg} and γ_{new}.

Taken together, the two approximation stages of the approximate update step transform the predicted posterior pdf $f(\tilde{X}_k, X_k|Z_{1:k-1})$ into an approximation of the new posterior pdf $f(\tilde{X}_k, X_k|Z_{1:k})$. This approximation is given by

$$\tilde{f}(\tilde{X}_k, X_k|Z_{1:k}) = \tilde{f}(\tilde{X}_k|Z_{1:k})\,\tilde{f}(X_k|Z_{1:k}),$$

where $\tilde{f}(\tilde{X}_k|Z_{1:k})$ is the LMB pdf in (21) and $\tilde{f}(X_k|Z_{1:k})$ is the Poisson pdf in (24). The update relations are (22) and (23) for the LMB parameters and (25) for the Poisson parameter. For general nonlinear/non-Gaussian system models, a sequential Monte Carlo (particle-based) implementation of the prediction and update steps of the LMB/P filter can be developed along the lines of [11].

VI. Experimental Study

A. Simulation Setup

We consider a two-dimensional (2D) region of interest (ROI) given by $[-150, 150] \times [-150, 150]$. The object states consist of 2D position and velocity, i.e, $\boldsymbol{x}_k = [x_{1,k}\ x_{2,k}\ \dot{x}_{1,k}\ \dot{x}_{2,k}]^{\text{T}}$. Their evolution is modeled as $\boldsymbol{x}_k = \boldsymbol{A}\boldsymbol{x}_{k-1} + \boldsymbol{W}\boldsymbol{u}_k$, where $\boldsymbol{A} \in \mathbb{R}^{4\times 4}$ and $\boldsymbol{W} \in \mathbb{R}^{4\times 2}$ are as in [15, Sec. 6.3.2] and $\boldsymbol{u}_k \sim \mathcal{N}(\boldsymbol{0}, \sigma_u^2\mathbf{I}_2)$ with $\sigma_u^2 = 0.01$ is an iid sequence of 2D Gaussian random vectors. Ten objects appear and disappear at various times before $k=30$ and after $k=140$, respectively; they move toward the ROI center and come in close proximity around $k=100$ [16, Sec. 9-A].

Within a measurement range of 300, a sensor produces measurements according to the nonlinear range-bearing model

$$\boldsymbol{z}_k = \big[\rho(\boldsymbol{x}_k)\ \theta(\boldsymbol{x}_k)\big]^{\text{T}} + \boldsymbol{v}_k ,$$

with $\rho(\boldsymbol{x}_k) \triangleq \|\boldsymbol{x}_k' - \boldsymbol{p}\|$ and $\theta(\boldsymbol{x}_k) \triangleq \tan^{-1}\big(\frac{x_{1,k}-p_1}{x_{2,k}-p_2}\big)$. Here, $\boldsymbol{x}_k' \triangleq [x_{1,k}\ x_{2,k}]^{\text{T}}$ is the object position, $\boldsymbol{p} = [p_1\ \ p_2]^{\text{T}} = [0\ \ -150]^{\text{T}}$ is the sensor position, and $\boldsymbol{v}_k$ is an iid sequence of 2D Gaussian random vectors whose components are independent with standard deviations $\sigma_\rho = 2$ and $\sigma_\theta = 1°$. The detection probability is $p_{\text{D}}\big(\boldsymbol{x}_k^{[l]}\big) = p_{\text{D}}(\boldsymbol{x}_k) = 0.5$. In addition, the sensor produces clutter with mean parameter $\mu_{\text{C}} = 20$ and a vector pdf $f_{\text{C}}(\boldsymbol{z}_k)$ that is linearly increasing on $[0, 300]$ and zero outside $[0, 300]$ with respect to the range component, and uniform on $[0°, 360°)$ with respect to the angle component; in Cartesian coordinates, this corresponds to a uniform distribution on the measurement range region.

We compare the performance of the proposed LMB/P filter with that of the PHD filter [4], [5], the LMB filter [9], and the TOMB/P filter [6], [11]; these filters will be briefly referred to as LMB/P, PHD, LMB, and TOMB/P, respectively. LMB/P represents the posterior PHD of unlabeled objects and the PHD of newborn unlabeled objects by 10.000 particles each; however, the resulting 20.000 particles are reduced to 10.000 particles after the update step. Similarly, PHD represents the posterior PHD and the PHD of newborn objects by 10.000 particles each, and reduces the resulting 20.000 particles to 10.000 particles after the update step. LMB/P, LMB, and TOMB/P use 1.000 particles to represent the vector pdfs of their Bernoulli components. TOMB/P represents the PHD of undetected objects by a grid with 40.000 cells [6]. LMB/P, LMB,[3] and TOMB/P calculate approximations of the marginal association pmfs by means of belief propagation [10], [12], [18]. PHD uses kmeans++ clustering [19] for state estimation. LMB/P, LMB, and TOMB/P declare an object as detected if the existence probability of the corresponding Bernoulli

[3]Our LMB implementation is based on an alternative derivation of the LMB update equations that involves an approximation of the object-measurement association pmf by the product of its marginals [17].

component exceeds 0.5, and then they calculate a state estimate as the weighted mean of the particles representing the corresponding vector pdf.

The birth PHD of LMB/P and PHD is chosen as a mixture of the pdfs

$$\tilde{f}_{\mathrm{B}}^{(m)}(\boldsymbol{x}_k) \propto \int f(\boldsymbol{x}_k|\boldsymbol{x}_{k-1})\, f\big(\boldsymbol{z}_{k-1}^{(m)}|x_{1,k-1}, x_{2,k-1}\big) \times f_{\mathrm{v}}(\dot{x}_{1,k-1}\ \dot{x}_{2,k-1})\, \mathrm{d}\boldsymbol{x}_{k-1}\,, \quad m = 1, \ldots, M_{k-1}\,,$$

where $f_{\mathrm{v}}(\dot{x}_{1,k}, \dot{x}_{2,k})$ is the pdf of independent, zero-mean, Gaussian random variables $\dot{\mathrm{x}}_{1,k}, \dot{\mathrm{x}}_{2,k}$ with variance 25. LMB creates a new Bernoulli component with vector pdf $s_{\mathrm{B}}^{(l)}(\boldsymbol{x}_k) = \tilde{f}_{\mathrm{B}}^{(m)}(\boldsymbol{x}_k)$, where $l = (k, m)$, for each $\boldsymbol{z}_{k-1}^{(m)}$. The mean number of newborn objects is $\mu_{\mathrm{B}} = 0.1$ for all filters. In TOMB/P, the vector pdf of newborn objects is uniform on the ROI. In LMB/P, the mean number of unlabeled objects is initialized (at time $k = 0$) by 0.01; in TOMB/P, the mean number of undetected objects is initialized by the same value. The thresholds used in LMB/P are $\gamma = 10^{-2}$, $\gamma_{\mathrm{leg}} = 10^{-5}$, and $\gamma_{\mathrm{new}} = 10^{-10}$. LMB uses threshold 10^{-3} for pruning Bernoulli components, and TOMB/P uses the same threshold for transferring Bernoulli components to the Poisson RFS [6].

B. Simulation Results

We measure the detection/tracking performance of the various filters by the mean optimal subpattern assignment (MOSPA) error with cutoff parameter $c = 20$ and order $p = 1$ [20], averaged over 1.000 Monte Carlo runs. Fig. 1(a) shows the MOSPA error versus time k. One can see that LMB/P, LMB, and TOMB/P perform similarly and substantially better than PHD. Fig. 1(b) shows the runtimes of our MATLAB implementations of the various filters on an Intel Xeon E5-2640 v3 CPU. LMB/P has the lowest runtime among the filters with similar MOSPA error (i.e., LMB/P, LMB, and TOMB/P). More specifically, its runtime is only 58.3% of that of LMB and 66.4% of that of TOMB/P. We note that the runtime of LMB/P can be further reduced—at the expense of a higher MOSPA error—by increasing γ and γ_{new}. Regarding γ_{leg}, we observed that a higher value increases the MOSPA error without reducing the runtime, while a lower value increases the runtime without reducing the MOSPA error.

We conclude from these results that for an appropriate choice of the thresholds γ, γ_{new}, and γ_{leg}, LMB/P is significantly less complex than both LMB and TOMB/P while exhibiting effectively the same detection/tracking performance.

VII. Conclusion

We proposed an efficient multiobject tracking algorithm that maintains track continuity. Our algorithm is based on a combination of labeled and unlabeled random finite sets (RFSs), and it achieves low complexity through several judiciously chosen approximations in the update step. Simulation results for a challenging scenario demonstrated an attractive accuracy-complexity tradeoff relative to other RFS-based multiobject tracking algorithms. An interesting direction of future research is an extension of our algorithm to multiple-detection measurement models and multisensor scenarios.

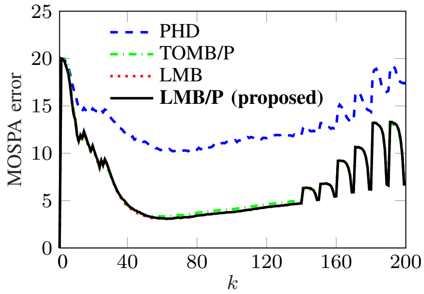

(a)

Filter	Runtime
PHD	0.0553 s
LMB/P	**0.1294 s**
TOMB/P	0.1949 s
LMB	0.2219 s

(b)

Fig. 1: Detection/tracking performance and computational complexity: (a) MOSPA error versus time k, (b) runtime per time (k) step.

References

[1] Y. Bar-Shalom, P. K. Willett, and X. Tian, *Tracking and Data Fusion: A Handbook of Algorithms*. Storrs, CT, USA: Yaakov Bar-Shalom, 2011.

[2] S. Challa, M. R. Morelande, D. Musicki, and R. Evans, *Fundamentals of Object Tracking*. Cambridge, UK: Cambridge University Press, 2011.

[3] W. Koch, *Tracking and Sensor Data Fusion: Methodological Framework and Selected Applications*. Berlin, Germany: Springer, 2014.

[4] R. P. S. Mahler, *Advances in Statistical Multisource-Multitarget Information Fusion*. Boston, MA, USA: Artech House, 2014.

[5] B.-N. Vo, S. Singh, and A. Doucet, "Sequential Monte Carlo methods for multitarget filtering with random finite sets," *IEEE Trans. Aerosp. Electron. Syst.*, vol. 41, no. 4, pp. 1224–1245, Apr. 2005.

[6] J. L. Williams, "Hybrid Poisson and multi-Bernoulli filters," in *Proc. FUSION-12*, Singapore, Jul. 2012, pp. 1103–1110.

[7] B.-T. Vo and B.-N. Vo, "Labeled random finite sets and multi-object conjugate priors," *IEEE Trans. Signal Process.*, vol. 61, no. 13, pp. 3460–3475, Jul. 2013.

[8] B.-N. Vo, B.-T. Vo, and D. Phung, "Labeled random finite sets and the Bayes multi-target tracking filter," *IEEE Trans. Signal Process.*, vol. 62, no. 24, pp. 6554–6567, Dec. 2014.

[9] S. Reuter, B.-T. Vo, B.-N. Vo, and K. Dietmayer, "The labeled multi-Bernoulli filter," *IEEE Trans. Signal Process.*, vol. 62, no. 12, pp. 3246–3260, Jun. 2014.

[10] J. L. Williams, "Marginal multi-Bernoulli filters: RFS derivation of MHT, JIPDA, and association-based MeMBer," *IEEE Trans. Aerosp. Electron. Syst.*, vol. 51, no. 3, pp. 1664–1687, Jul. 2015.

[11] T. Kropfreiter, F. Meyer, and F. Hlawatsch, "Sequential Monte Carlo implementation of the track-oriented marginal multi-Bernoulli/Poisson filter," in *Proc. FUSION-16*, Heidelberg, Germany, Jul. 2016, pp. 972–979.

[12] F. Meyer, T. Kropfreiter, J. L. Williams, R. A. Lau, F. Hlawatsch, P. Braca, and M. Z. Win, "Message passing algorithms for scalable multitarget tracking," *Proc. IEEE*, vol. 106, no. 2, pp. 221–259, Feb. 2018.

[13] D. Daley and D. Vere-Jones, *An Introduction to the Theory of Point Processes, Vol. I*. New York, NY, USA: Springer, 2003.

[14] R. L. Streit, *Poisson Point Processes — Imaging, Tracking and Sensing*. New York, NY, USA: Springer, 2010.

[15] Y. Bar-Shalom, X.-R. Li, and T. Kirubarajan, *Estimation with Applications to Tracking and Navigation*. New York, NY, USA: Wiley, 2002.

[16] F. Meyer, P. Braca, P. Willett, and F. Hlawatsch, "A scalable algorithm for tracking an unknown number of targets using multiple sensors," *IEEE Trans. Signal Process.*, vol. 65, no. 13, pp. 3478–3493, Jul. 2017.

[17] T. Kropfreiter and F. Hlawatsch, "A fast labeled multi-Bernoulli filter based on belief propagation," *IEEE Trans. Aerosp. Electron. Syst.*, submitted, 2018.

[18] J. L. Williams and R. Lau, "Approximate evaluation of marginal association probabilities with belief propagation," *IEEE Trans. Aerosp. Electron. Syst.*, vol. 50, no. 4, pp. 2942–2959, Oct. 2014.

[19] G. Gan, C. Ma, and J. Wu, *Data Clustering: Theory, Algorithms, and Applications*. Philadelphia, PA, USA: SIAM, 2007.

[20] D. Schuhmacher, B.-T. Vo, and B.-N. Vo, "A consistent metric for performance evaluation of multi-object filters," *IEEE Trans. Signal Process.*, vol. 56, no. 8, pp. 3447–3457, Aug. 2008.